Robustness and enhancement of neural synchronization by activity-dependent coupling

V. P. Zhigulin,[1,2,*] M. I. Rabinovich,[2] R. Huerta,[2,3] and H. D. I. Abarbanel[2,4]
[1]*Department of Physics, MC 103-33, California Institute of Technology, Pasadena, California 91125*
[2]*Institute for Nonlinear Science, University of California, San Diego, La Jolla, California 92093-0402*
[3]*GNB, ETS de Ingeniería Informática, Universidad Autónoma de Madrid, 28049 Madrid, Spain*
[4]*Department of Physics and Marine Physical Laboratory (Scripps Institution of Oceanography), University of California, San Diego, La Jolla, California 93093-0402*

(Received 7 February 2002; revised manuscript received 3 October 2002; published 6 February 2003)

We study the synchronization of two model neurons coupled through a synapse having an activity-dependent strength. Our synapse follows the rules of spike-timing dependent plasticity. We show that this plasticity of the coupling between neurons produces enlarged frequency-locking zones and results in synchronization that is more rapid and much more robust against noise than classical synchronization arising from connections with constant strength. We also present a simple discrete map model that demonstrates the generality of the phenomenon.

DOI: 10.1103/PhysRevE.67.021901 PACS number(s): 87.18.Sn, 87.18.Bb, 05.45.Xt

Synchronous activity among individual neurons or their ensembles is a robust phenomenon observed in many regions of the brain, in sensory systems and in other neural networks. With constant synaptic connections, the regions of neural synchronization are quite narrow in parameter space and the origin of the observed robustness of synchronization is not clear. It is known that many neurons in the cortex, in the cerebellum, and in other neural systems are coupled through excitatory synaptic connections whose strength can be altered through activity-dependent plasticity. Indeed, this plasticity is widely thought to underlie learning processes, and in itself constitutes a broadly interesting phenomenon. Here we discuss its role in the synchronization of neurons in a network.

There have been recent experimental advances in the understanding of such plasticity, and, in particular, of the critical dependence on timing in presynaptic and postsynaptic signaling. Two manifestations of this kind of synaptic plasticity are the spike-timing dependent plasticity (STDP) [1,2], seen in excitatory connections between neurons, and its inverse, observed, for example, in the connections between excitatory and inhibitory neurons in the electrosensory lobe of fish [3]. The connections between excitatory neurons through inhibitory interneurons are typical in sensory systems [4,5] and the cerebral cortex [6]. These also express synaptic plasticity [7] and play an important role in the control and synchronization of neural ensembles in the hippocampus.

We report here on the synchronization of two model neurons coupled through STDP or inverse STDP synapses. We demonstrate that such coupling leads to neural synchronization that is more rapid, more flexible, and much more robust against noise than synchronization mediated by constant strength connections. (For reviews, see [8–10].) We also build a simple discrete map that illustrates the enhancement of synchronization by activity-dependent coupling. The map allows us to speculate about the general applicability of learning-enhanced synchronization.

We consider here the simplest neural network: two neurons with unidirectional, activity-dependent excitatory synaptic coupling. Each neuron is described by the Hodgkin-Huxley equations with standard Na, K, and ''leak'' currents [11],

$$C\frac{dV_i(t)}{dt} = -g_{\mathrm{Na}} m_i(t)^3 h_i(t)[V_i(t)-E_{\mathrm{Na}}] - g_{\mathrm{K}} n_i(t)^4 \times [V_i(t)-E_{\mathrm{K}}] - g_L[V_i(t)-E_L] - I_{\mathrm{syn}}(t) + I_{\mathrm{stim}}, \tag{1}$$

where $i=1,2$.

Each of the activation and inactivation variables $y_i(t) = \{n_i(t), m_i(t), h_i(t)\}$ satisfies first-order kinetics,

$$\frac{dy_i(t)}{dt} = \alpha_y[V_i(t)][1-y_i(t)] - \beta_y[V_i(t)]y_i(t). \tag{2}$$

The parameters in these equations are given in [12].

Each neuron receives a constant input I_{stim} forcing it to spike with a constant I_{stim}-dependent frequency. The second neuron is synaptically driven by the first via an excitatory current dependent on the postsynaptic $V_2(t)$ and presynaptic $V_1(t)$ membrane voltages,

$$I_{\mathrm{syn}}(t) = g(t)S(t)V_2(t). \tag{3}$$

$S(t)$ is the fraction of open synaptic channels. It satisfies first-order kinetics,

$$\frac{dS(t)}{dt} = \alpha[1-S(t)]H(V_1(t)) - \beta S(t), \tag{4}$$

with $H(V_1(t)) = \{1+\tanh[10V_1(t)]\}/4$.

The time-dependent synaptic coupling strength $g(t)$ is conditioned by the dynamics of the presynaptic and postsynaptic neurons. We consider two types of activity-dependent couplings: (i) an excitatory synapse with STDP, and (ii) an

*Electronic address: zhigulin@caltech.edu

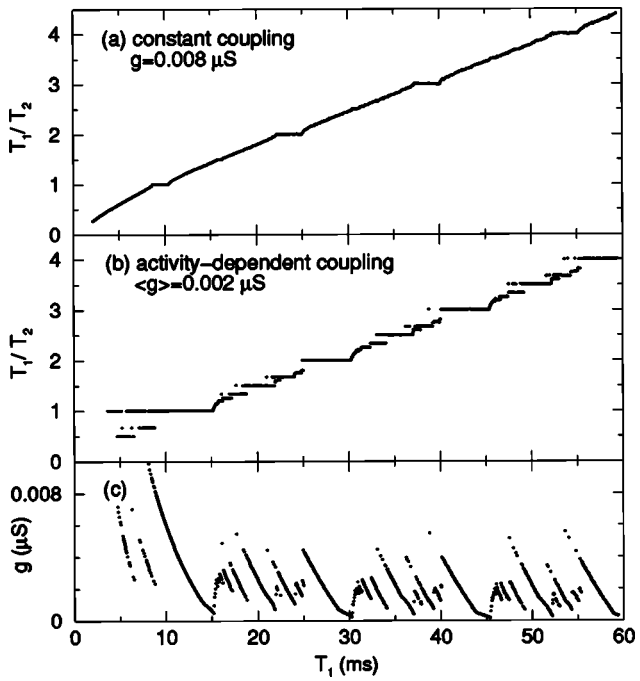

FIG. 1. Devil's staircase for (a) constant synaptic strength and (b) synaptic strength varying according to inverse STDP coupling. T_1 and T_2 are the observed periods of the presynaptic (driving) neuron and postsynaptic (driven) neuron, respectively. In (c) the final value of synaptic strength is displayed.

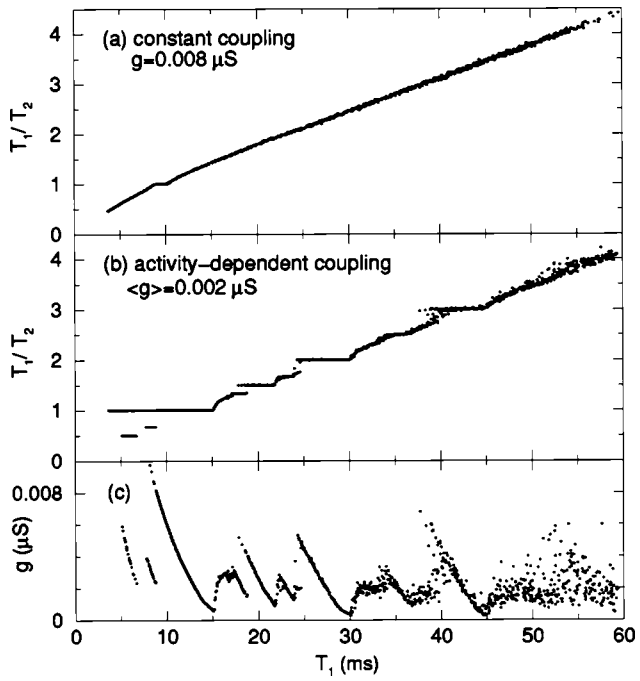

FIG. 2. Same as Fig. 1, but with zero mean, Gaussian, white noise with $\sigma=0.1$ nA added to the membrane currents.

excitatory synapse with inverse STDP. Through STDP $g(t)$ changes by $\Delta g(t)$, which is a function of the time difference $\Delta t = t_{\text{post}} - t_{\text{pre}}$ between the times of postsynaptic and presynaptic spikes. We use the additive update rule

$$\Delta g(t) = G(\Delta t) = A \text{sgn}(\Delta t) \exp(-\gamma|\Delta t|) \tag{5}$$

for STDP and $\Delta g(t) = -G(\Delta t)$ for inverse STDP. We used $A=0.004$ μS and $\gamma = 0.15$ ms^{-1}.

We studied the synchronization properties of this coupled system by setting the autonomous period of the postsynaptic neuron to 15 ms, then evaluating the actual period of its oscillation T_2 as a function of the imposed autonomous oscillation period T_1 of the presynaptic neuron. In Fig. 1, we show T_1/T_2 as a function of T_1 in two cases: (a) a synaptic coupling with constant strength 0.008 μS and (b) a synaptic coupling with inverse STDP. In the latter case, the steady-state coupling strength depends on the ratio of neuronal frequencies (c). Its average over all T_1 values is 0.002 μS, which is much lower than the strength in the case of constant coupling.

In Fig. 1(a), we see the familiar ''devil's staircase'' associated with frequency-locking domains of a driven nonlinear oscillator. Only frequency locking with ratios 1:1, 2:1, 3:1, and 4:1 leads to synchronization plateaus with significant width. In Fig. 1(b), we see that the synchronization domains are substantially broadened due to activity-dependent coupling, especially for $T_1/T_2=1$. Some synchronization plateaus exhibit multistability, which we confirmed by observing the associated hysteresis. These results show that even a weak but adaptive connection with strength that is determined dynamically is able to greatly enhance and enrich synchronization.

We also studied the robustness of this enhanced synchronization in the presence of noise by adding zero mean, Gaussian, white noise to the membrane currents of each neuron. We examined the behavior of the system with RMS noise amplitudes $\sigma=0.01$, 0.05, 0.1, and 0.5 nA.

For $\sigma=0.01$ nA, no phase-locking plateaus were destroyed. At $\sigma=0.05$ nA, the 4:1 plateau became distorted. Larger σ sequentially eliminated synchronization plateaus until only the 1:1 plateau remained. The 1:1 plateau was seen for all σ. In Fig. 2, we illustrate the effect of the noise on synchronization when $\sigma=0.1$ nA with (a) constant and (b) inverse STDP coupling. While in (a) most of the plateaus have disappeared, in (b) the 1:1, the 2:1, and even the 3:1 frequency-locking regimes remained. In sharp distinction to classical synchronization, frequency locking through activity-dependent coupling is significantly more robust in the presence of noise.

To understand the mechanisms behind such a remarkable robustness, we studied the diffusion of oscillation phase caused by noise. For $\sigma=0.5$ nA, in Fig. 3(a) we show that in the case of 1:1 synchronization and coupling with constant strength 0.008 μS, noise-induced phase diffusion results in 2π phase slips that destroy synchronized state. Quite to the contrary, Fig. 3(b) shows that in the case of activity-dependent coupling, phase slips are absent and the phase difference does not increase. In this particular case, the strength of coupling varied around the mean of 0.0064 μS with a standard deviation of 0.0026 μS.

In Fig. 4, we plot the average rate of phase slips for different amplitudes of the noise. In line with the above obser-

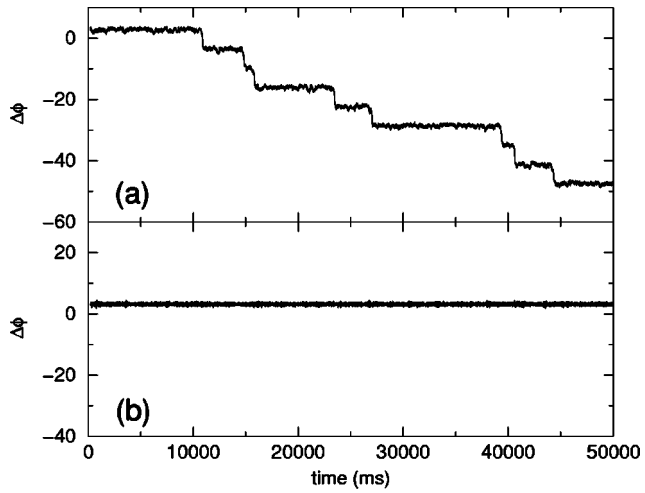

FIG. 3. The difference of oscillation phases of two neurons as a function of time in the cases of (a) constant and (b) activity-dependent coupling.

vation, we see that in the case of activity-dependent coupling (dashed line), phase slips are suppressed in a wide range of noise amplitudes. We argue here that this suppression of phase slips is the primary mechanism responsible for robustness of synchronization mediated by activity-dependent coupling. After the introduction of a discrete map model, we will discuss this mechanism in more detail.

We also considered synchronization through an activity-dependent synapse in the interesting case in which the presynaptic neuron produces bursts of spikes and the postsynaptic neuron spikes irregularly. We found that synchronization through an STDP synapse is very fast; even a few spikes are enough for the frequency locking to establish itself. Neurons in the same setup with constant coupling synchronize much more slowly and *only* if the strength of the connection is appropriate for the given ratio of their frequencies. Hence, activity-dependent synapses allow adaptation ''on the run,'' synching a postsynaptic neuron to the firing properties of its presynaptic partner.

To understand the above results in a general way, we have constructed a discrete time map model of periodic generators with STDP-like coupling. This map accounts for the dependence of the coupling strength on the activity of generators.

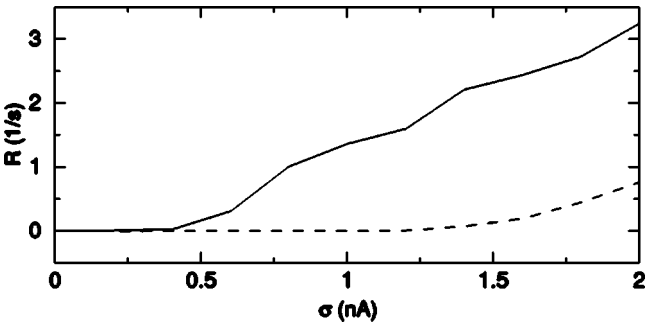

FIG. 4. Average rate of phase slips as a function of rms noise amplitude for the case of 1:1 synchronization and constant (solid line) or activity-dependent (dashed line) coupling.

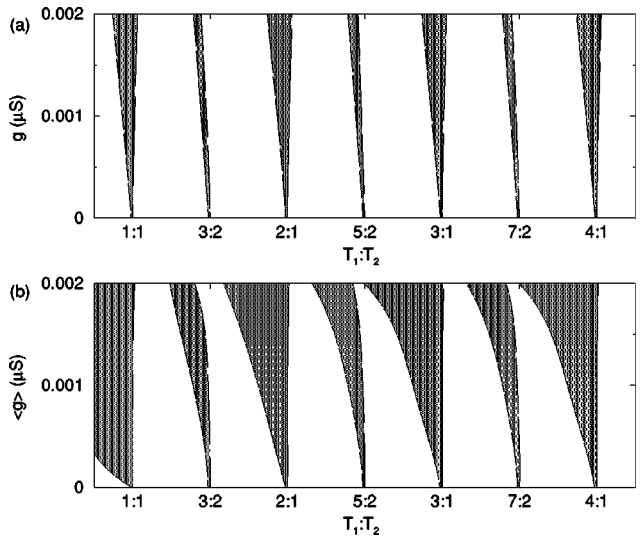

FIG. 5. Arnol'd tongues calculated for the discrete map model with (a) constant and (b) activity-dependent coupling. $T_2^0=13$ ms.

Take T_1^0 and T_2^0 as the autonomous periods of the first and second generators. As a result of unidirectional coupling, the period of the second generator will change by some amount ΔT each time it receives a spike from the first generator. Assuming initial phases to be 0, the times of the $(n+1)$st spike of the first generator and the $(m+1)$st spike of the second generator are taken to satisfy

$$t_{n+1}^{(1)}=t_n^{(1)}+T_1^0, \tag{6a}$$

$$t_{m+1}^{(2)}=t_m^{(2)}+T_2^0-\Delta T_{m,n}, \tag{6b}$$

where n and m are such that $t_m^{(2)}\leqslant t_n^{(1)}\leqslant t_{m+1}^{(2)}$. In general, $\Delta T_{m,n}$ would be a function of T_1^0, T_2^0, $t_n^{(1)}$, $t_m^{(2)}$, and the coupling strength $g_{m,n}$. We argue that the two main variables here are $t_n^{(1)}-t_m^{(2)}$ and $g_{m,n}$. In the simplest case, $\Delta T_{m,n}$ can be approximated by

$$\Delta T_{m,n}=g_{m,n}F(t_n^{(1)}-t_m^{(2)}), \tag{7}$$

where the function $F(x)$ is the analog of a phase response curve [13] for our model. To obtain results quantitatively comparable with our neuronal model, we fit it by a non-negative quadratic function that describes the phase response of our model neurons: $F(x)=835+63x-9x^2$ for $0\leqslant x\leqslant T_2^0$ and 0 otherwise. $g_{m,n}$ obeys the inverse STDP update rules,

$$g_{m+1,n}=g_{m,n}-G(t_{m+1}^{(2)}-t_n^{(1)}), \tag{8a}$$

$$g_{m,n}=g_{m,n-1}-G(t_m^{(2)}-t_n^{(1)}). \tag{8b}$$

In Fig. 5, we show the Arnol'd tongues calculated for the map (6a)–(8b) in the cases of (a) constant and (b) inverse STDP coupling. As with the model neurons, we see that activity-dependent coupling greatly enlarges the zones of synchronization.

This discrete map can be further analyzed to find its fixed points corresponding to $n:m$ synchronization and to examine

their stability. We present here only the case of 1:1 synchronization. Then $m=n$, and the system of equations (6)–(8) can be written in the following simple form:

$$\tau_{n+1}=\tau_n+T_1^0-T_2^0+g_nF(\tau_n), \tag{9a}$$

$$g_{n+1}=g_n-G(T_1^0-\tau_{n+1})-G(-\tau_{n+1}), \tag{9b}$$

where $\tau_n=t_n^{(1)}-t_n^{(2)}$. The fixed points of Eqs. (9) are given by $g_n^f=(T_2^0-T_1^0)/F(\tau_n^f)$ and $\tau_n^f=T_1^0/2$. Stability calculations show that for such $F(\tau)$ and $G(\tau)$ these fixed points are stable. The second fixed point illustrates that activity-dependent coupling introduces a new limitation on the relationship between the phases of two oscillators. It is this limitation that causes the suppression of phase slips under the influence of noise. Detailed analysis shows that in the course of noise-affected synchronization, the strength of activity-dependent coupling adjusts dynamically to keep this phase relationship close to satisfaction and, hence, suppresses phase slips.

In conclusion, we have analyzed the effects of activity-dependent coupling on synchronization properties of coupled neurons. We showed that such coupling results in a substantial extension of the temporal synchronization zones, leads to more rapid synchronization, and makes it much more robust against noise. The enlargement of synchronization zones means that with STDP-like learning rules, the number of synchronized neurons in a large heterogeneous population must increase. In fact, this is an aspect of the popular idea due to Hebb [14]. It is supported by the results in [15,16], which indicate that the coherence of fast EEG activity in the gamma band increases in a process of associative learning.

Based on our discrete map model results, we argue that the particular details of the signal-generating devices (e.g., neurons) and their connections (e.g., synapses) are not essential and the obtained results have general applicability. In fact, we observed similar phenomena of robust and enhanced synchronization in computer simulations of other types of periodic generators (such as Van-der-Pol and θ oscillators) with STDP-like activity-dependent coupling.

ACKNOWLEDGMENTS

This work was partially supported by U.S. Department of Energy Grant Nos. DE-FG03-90ER14138 and DE-FG03-96ER14592, NSF Grant Nos. PHY0097134 and EIA-0130708, Army Research Office Grant No. DAAD19-01-1-0026, Office of Naval Research Grant No. N00014-00-1-0181, and NIH Grant No. R01 NS40110-01A2. R.H. thanks MCyT (Spain) for Grant No. BFI2000-0157.

[1] H. Markram, J. Lubke, M. Frotscher, and B. Sakmann, Science **275**, 213 (1997).
[2] G.-Q. Bi and M.-M. Poo, J. Neurosci. **18**, 10464 (1998).
[3] C. Bell, V. Han, Y. Sugavara, and K. Grant, J. Exp. Biol. **202**, 1339 (1999).
[4] G. Laurent, Science **286**, 723 (1999).
[5] M. Rabinovich, A. Volkovskii, P. Lecanda, R. Huerta, H. Abarbanel, and G. Laurent, Phys. Rev. Lett. **87**, 068102 (2001).
[6] M. Bear and D. Linden, in *Synapses*, edited by W.M. Cowan, T.C. Sdhof, and C.F. Stevens (Johns Hopkins University Press, Baltimore, MD, 2001), p. 455.
[7] Y. Perez, F. Morin, and J.-C. Lacaille, Proc. Natl. Acad. Sci. U.S.A. **98**, 9401 (2001).
[8] L. Glass, Nature (London) **410**, 277 (2001).
[9] R. Elson, A. Selverston, R. Huerta, N. Rulkov, M. Rabinovich, and H. Abarbanel, Phys. Rev. Lett. **81**, 5692 (1998).
[10] S. Coombes and P. Bressloff, Phys. Rev. E **60**, 2086 (1999).
[11] R. D. Traub and R. Miles, *Neuronal Networks of the Hippocampus* (Cambridge University Press, New York, 1991), Chap. 4.
[12] The following values were used: $g_L=0.027$ μS, $E_L=-64$ mV, $E_{\mathrm{Na}}=50$ mV, $g_{\mathrm{Na}}=7.15$ μS, $g_{\mathrm{K}}=1.43$ μS, $E_{\mathrm{K}}=-95$ mV, $\alpha=10$ ms^{-1}, $\beta=0.2$ ms^{-1}, $C=1.43\times10^{-4}$ μF, $\alpha_n=0.032(-50-V)/\{\exp[(-50-V)/5]-1\}$; $\beta_n=0.5\exp[(-55-V)/40]$, $\alpha_m=0.32(-52-V)/\{\exp[(-52-V)/4]-1\}$, $\beta_m=0.28(25+V)/\{\exp[(25+V)/5]-1\}$, $\alpha_h=0.128\exp[(-48-V)/18]$, and $\beta_h=4/\{\exp[(-25-V)/5]+1\}$.
[13] A. Winfree, *The Geometry of Biological Time* (Springer-Verlag, New York, 1980).
[14] D. Hebb, *The Organization of Behavior* (Wiley, New York, 1949).
[15] W. Miltner, C. Braun, M. Arnold, H. Witte, and E. Traub, Nature (London) **397**, 434 (1999).
[16] J. Fell, P. Klaver, K. Lehnertz, T. Grunvald, C. Schaller, C. Elgar, and G. Fernandez, Nat. Neurosci. **4**, 1259 (2001).